sized with sodium pentobarbital. A silver clip (0.2 mm in diameter) was placed on the left renal artery in the preparation of the renal hypertensive rats. In the preparation of the DOCA-salt hypertensive rats, the left kidney was removed and a DOCA pellet (50 mg) was implanted subcutaneously. The DOCA rats were then fed an 8% salt diet. Rats from both groups were used after 8 weeks in the experiments, together with male, 17–22-week old spontaneous hypertensive rats. The average systolic pressure in these groups of hypertensive rats ranged from 209 to 237 mm Hg, and no significant difference was found between groups. Eight-week-old male Wistar rats were used as controls. Their average systolic pressure was 139 mm Hg. Y-27632 was administered orally. The systolic blood pressure was measured by the tail cuff method at 1, 3, 5, 7 and 24 h. The rats were prewarmed to 40 °C for 10 min before each measurement. No toxicity was found in rats treated with 30 mg kg^{-1} of Y-27632 administered *per os* once per day for 10 days.

Received 3 June; accepted 13 August 1997.

1. Somlyo, A. P. & Somlyo, A. V. Signal transduction and regulation in smooth muscle. *Nature* **372,** 231–236 (1994).
2. Somlyo, A. P. *et al.* Modulation of Ca^{2+}-sensitivity and of the time course of contraction in smooth muscle: A major role of protein phosphatase? *Adv. Prot. Phosphat.* **5,** 181–195 (1989).
3. Kitazawa, T., Masuo, M. & Somlyo, A. P. G Protein-mediated inhibition of myosin light-chain phosphatase in vascular smooth muscle. *Proc. Natl Acad. Sci. USA* **88,** 9307–9310 (1991).
4. Hirata, K. *et al.* Involvement of rho p21 in the GTP-enhanced calcium ion sensitivity of smooth muscle contraction. *J. Biol. Chem.* **267,** 8719–8722 (1992).
5. Gong, M. C. *et al.* Role of guanine nucleotide-binding proteins, ras-family or trimeric proteins or both in Ca^{2+} sensitization of smooth muscle. *Proc. Natl Acad. Sci. USA* **93,** 1340–1345 (1996).
6. Kimura, K. *et al.* Regulation of myosin phosphatase by Rho and Rho-associated kinase (Rho-kinase) *Science* **273,** 245–248 (1996).
7. Ishizaki, T. *et al.* The small GTP-binding protein Rho binds to and activates a 160 kDa Ser/Thr protein kinase homologous to myotonic dystrophy kinase. *EMBO J.* **15,** 1885–1893 (1996).
8. Kitazawa, T., Kobayashi, S., Horiuti, K., Somlyo, A. V. & Somlyo, A. P. Receptor-coupled, permeabilized smooth muscle. *J. Biol. Chem.* **264,** 5339–5342 (1989).
9. Ishihara, H. *et al.* Calyculin A and okadaic acid: inhibitors of protein phosphatase activity. *Biochem. Biophys. Res. Commun.* **159,** 871–877 (1989).
10. Saitoh, M., Ishikawa, T., Matushima, S., Naka, M. & Hidaka, H. Selective inhibition of catalytic activity of smooth muscle myosin light chain kinase. *J. Biol. Chem.* **262,** 7796–7801 (1987).
11. Leung, T., Manser, E., Tan, L. & Lim, L. A novel serine/threonine kinase binding the Ras-related RhoA GTPase which translocates the kinase to peripheral membranes. *J. Biol. Chem.* **270,** 29051–29054 (1995).
12. Matsui, T. *et al.* Rho-associated kinase, a novel serine threonine kinase, as a putative target for the small GTP binding protein Rho. *EMBO J.* **15,** 2208–2216 (1996).
13. Nakagawa, O. *et al.* ROCK-I and ROCK-II; two isoforms of Rho-associated coiled-coil forming protein serine/threonine kinase in mice. *FEBS Lett.* **392,** 189–193 (1996).
14. Manser, E. *et al.* A brain serine/threonine protein kinase activated by Cdc42 and Rac1. *Nature* **367,** 40–46 (1994).
15. Ridley, A. J. & Hall, A. The small GTP-binding protein rho regulates the assembly of focal adhesions and actin stress fibers in response to growth factors. *Cell* **70,** 389–399 (1992).
16. Ishizaki, T. *et al.* p160ROCK, a Rho-associated coiled-coil forming protein kinase, works downstream of Rho and induces focal adhesions. *FEBS Lett.* **404,** 118–124 (1997).
17. Leung, T., Chen, X.-Q., Manser, E. & Lim, L. The p160 RhoA-binding kinase ROKα is a member of a kinase family and is involved in the reorganization of the cytoskeleton. *Mol. Cell. Biol.* **16,** 5313–5327 (1996).
18. Amano, M. *et al.* Formation of actin stress fibres and focal adhesions enhanced by Rho-kinase. *Science* **275,** 1308–1311 (1997).
19. Narumiya, S. The small GTPase Rho: cellular functions and signal transduction. *J. Biochem.* **120,** 215–228 (1996).
20. Ridley, A. J., Paterson, H. F., Johnston, C. L., Diekmann, D. & Hall, A. The small GTP-binding protein rac regulates growth factor-induced membrane ruffling. *Cell* **70,** 401–410 (1992).
21. Tapon, N. & Hall, A. Rho, Rac and Cdc42 GTPases regulate the organization of the actin cytoskeleton. *Curr. Opin. Cell Biol.* **9,** 86–92 (1997).
22. Satoh, H. & Inui, J. Endothelial cell-dependent relaxation and contraction induced by histimine in the isolated guinea-pig pulmonary artery. *Eur. J. Pharmacol.* **97,** 321–324 (1984).
23. Kobayashi, S., Kitazawa, T., Somlyo, A. V. & Somlyo, A. P. Cytosolic heparin inhibits muscarinic and α-adrenergic Ca^{2+} release in smooth muscle. *J. Biol. Chem.* **264,** 17997–18004 (1989).
24. Bagrodia, S. *et al.* Identification of a mouse $p21^{Cdc42/Rac}$ activated kinase. *J. Biol. Chem.* **270,** 22731–22737 (1995).
25. Kikkawa, U., Takai, Y., Minakuchi, R., Inohara, S. & Nishizuka, Y. calcium-activated, phospholipid-dependent protein kinase from rat brain. Subcellular distribution, purification and properties. *J. Biol. Chem.* **257,** 13341–13348 (1982).
26. Adelstein, R. S. & Klee, C. B. Purification of smooth muscle myosin light chain kinase. *Meth. Enzym.* **85,** 298–308 (1985).
27. Takayasu, M. *et al.* The effects of HA compound calcium antagonists on delayed cerebral vasospasm in dogs. *J. Neurosurg.* **65,** 80–85 (1986).
28. Hidaka, H., Inagaki, M., Kawamoto, S. & Sasaki, Y. Isoquinolinesulfonamides, novel and potent inhibitors of cyclic nucleotide dependent protein kinase and protein kinase C. *Biochemistry* **9,** 5036–5041 (1984).
29. Bubin, C. S., Erlichman, J. & Rosen, O. M. Cyclic AMP-dependent protein kinase from bovine heart muscle. *Meth. Enzymol.* **38,** 308–315 (1974).

Acknowledgements. We thank S. Ohno and R. Cerione for recombinant PKCε and PAK cDNA, respectively, H. Karaki for helpful suggestions, H. Bito for critical reading of the manuscript, and K. Okuyama for secretarial assistance. Supported in part by a grant-in-aid for specially promoted research from the Ministry of Education, Science and Culture of Japan, and by an HFSP grant.

Correspondence and requests for materials should be addressed to M.U. (e-mail: uehata@yoshitomi.co.jp) or S.N. (e-mail: snaru@mfour.med.kyoto-u.ac.jp).

The Fork head transcription factor DAF-16 transduces insulin-like metabolic and longevity signals in *C. elegans*

Scott Ogg, Suzanne Paradis, Shoshanna Gottlieb, Garth I. Patterson, Linda Lee, Heidi A. Tissenbaum & Gary Ruvkun

Department of Molecular Biology, Massachusetts General Hospital, Department of Genetics, Harvard Medical School, Boston, Massachusetts 02114, USA

In mammals, insulin signalling regulates glucose transport together with the expression and activity of various metabolic enzymes. In the nematode *Caenorhabditis elegans*, a related pathway regulates metabolism, development and longevity[1,2]. Wild-type animals enter the developmentally arrested dauer stage in response to high levels of a secreted pheromone[3], accumulating large amounts of fat in their intestines and hypodermis. Mutants in DAF-2 (a homologue of the mammalian insulin receptor) and AGE-1 (a homologue of the catalytic subunit of mammalian phosphatidylinositol 3-OH kinase) arrest development at the dauer stage[3]. Moreover, animals bearing weak or temperature-sensitive mutations in *daf-2* and *age-1* can develop reproductively, but nevertheless show increased energy storage and longevity[1,2,4,5]. Here we show that null mutations in *daf-16* suppress the effects of mutations in *daf-2* or *age-1*; lack of *daf-16* bypasses the need for this insulin receptor-like signalling pathway. The principal role of DAF-2/AGE-1 signalling is thus to antagonize DAF-16. *daf-16* is widely expressed and encodes three members of the Fork head family of transcription factors. The DAF-2 pathway acts synergistically with the pathway activated by a nematode TGF-β-type signal, DAF-7, suggesting that DAF-16 cooperates with nematode SMAD proteins in regulating the transcription of key metabolic and developmental control genes. The probable human orthologues of DAF-16, FKHR and AFX, may also act downstream of insulin signalling and cooperate with TGF-β effectors in mediating metabolic regulation. These genes may be dysregulated in diabetes.

The metabolic, longevity, and developmental defects caused by *daf-2* and *age-1* mutations are suppressed by *daf-16* mutations[5,6] (Fig. 1 and Table 1). Wild-type animals do not arrest at the dauer stage in low pheromone, whereas temperature-sensitive mutations in *daf-2* cause 100% arrest at the dauer larval stage (Table 1). *daf-2* mutant animals also shift metabolism towards fat accumulation and show large drops of fat in the intestine and hypodermis of dauer larvae, as measured by Sudan black staining (Fig. 1a). However, animals bearing both a *daf-2* mutation and the *daf-16*(*mgDf47*) or *daf-16*(*mgDf50*) null mutations (see below) do not arrest at the dauer stage or store large amounts of fat, developing instead into reproductive adults (Table 1 and Fig. 1b). Therefore, *daf-16* is a major target of DAF-2/AGE-1 signalling.

A parallel DAF-7 TGF-β pathway also regulates *C. elegans* metabolism and development[3]. *daf-16* gene activity is not necessary for the metabolic shift towards energy storage or dauer arrest induced by lack of DAF-7 TGF-β signalling (Fig. 1c). For example, like *daf-7*(*e1372*) mutant animals, *daf-16*(*mgDf50*); *daf-7*(*e1372*) mutant animals arrest at the dauer stage (172/174 animals arrest) and accumulate fat. The arrest, however, is not complete. The pharynx is not contracted (2/100 arrested animals have a constricted pharynx) and the intestine is less refractile than normal dauers, as has been reported using the *daf-16*(*m26*) allele[7] (see below). Thus

Table 1 Effect of *daf-16* null mutations on dauer formation

Genotype	Phenotype of progeny at 25 °C (%)				
	L4 and adults	Dauer	Dead eggs	Other*	*N*†
N2 Bristol (wild type)	98.6	0	0.3	1.1	721
daf-2(*e1370*)	0	95.2	2.8	2.0	714
daf-16(*mgDf50*)	79.6	0	18.1	2.3	348
daf-16(*mgDf47*); *daf-2*(*e1370*)	84.1	0	10.2	5.7	422
daf-16(*mg50*); *daf-2*(*e1370*)	95.1	0	3.5	1.4	833
daf-16(*mg54*); *daf-2*(*e1370*)	89.6	0.4‡	9.2	0.8	502
daf-3(*mgDf90*)	98.6	0	ND	1.4	737
daf-2(*e1370*); *daf-3*(*mgDf90*)	0	97	ND	3.0	934
Pheromone + wild type	64.2	35.8	ND	0	1,121
Pheromone + *daf-16*(*mgDf50*)	73.9	23.9‡	ND	2.2	742
Pheromone + *daf-3*(*mgDf90*)	61.0	37.7	ND	1.3	899
Pheromone + *daf-16*(*mgDf50*); *daf-3*(*mgDf90*)	56.1	41.8‡	ND	2.1	743

* 'Other' includes animals that could not be classified as dauer or non-dauer because the animal was young, had grossly aberrant morphology, or was dead.
† *N*, total number of animals scored.
‡ Under these conditions the dauers were not fully formed. These larvae were similar to dauers in having a shrunken cuticle, but the pharynx pumped and was not shrunken, the intestine was not dark and alae were indistinct.

placement of *daf-16* in the insulin receptor-like genetic pathway and not the DAF-7 TGF-β-like pathway is confirmed with a null *daf-16* allele. In support of the parallel pathway model, the *daf-3*(*mgDf90*) null mutation, which potently suppresses *daf-7*(*e1372*) (ref. 8), does not suppress *daf-2*(*e1370*) (Table 1 and Fig. 1d).

daf-16 and *daf-3* do not represent the only output of pheromone signalling. *daf-16*(*mgDf50*) animals arrest at the dauer stage in dauer pheromone, although the arrested animals are partial dauers, with large pharynxes and low refractility (Table 1; see below). *daf-3*(*mgDf90*) single mutants form apparently normal dauers in the presence of pheromone (Table 1). *daf-16*; *daf-3* double-null mutant animals arrest as partial dauers in dauer pheromone, like the *daf-16* single mutant (Table 1). Thus, *daf-16* gene activity is necessary for some aspects of dauer arrest, and other pathways besides those coupled to *daf-3* and *daf-16*, for example the pathways defined by *daf-11* or *daf-12* (ref. 3), may also regulate arrest at the dauer stage in pheromone. *daf-16* and *daf-3* have no obvious function during reproductive development. Reproductively growing animals bearing null mutations in either *daf-16* or *daf-3*, or mutations in both genes do not dramatically alter fat accumulation in larvae or adult animals compared to wild type (data not shown).

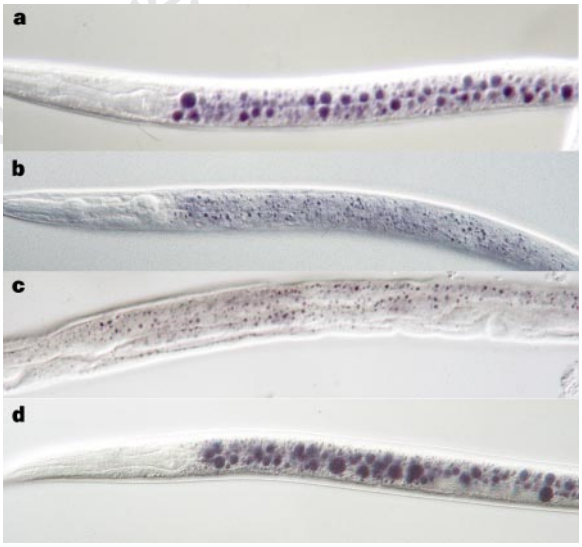

Figure 1 Metabolic control by *daf-16* and *daf-3*. Fat accumulation assayed by Sudan black in dauer larval stage and the comparable reproductive larval stage 3 and 4 in animals grown at 25 °C. **a**, *daf-2*(*e1370*). **b**, Suppression of fat accumulation in *daf-16*(*mgDf50*); *daf-2*(*e1370*) animals. **c**, Suppression of *daf-7*(*e1372*) fat storage and arrest by *daf-3*(*mgDf90*). **d**, *daf-16*(*mgDf50*) mutant does not suppress the fat accumulation or arrest of a *daf-7*(*e1372*) mutant.

We genetically mapped *daf-16* to a 300-kilobase cosmid and YAC contig (Fig. 2a). Multiple *daf-16* mutations induced with γ rays or ethylmethane sulphonate (EMS) were isolated as suppressors of the dauer constitutive phenotype induced by the *daf-2*(*e1370*) mutant. DNAs isolated from these *daf-16* alleles were surveyed for deletions or rearrangement breakpoints using cosmids in this contig (Fig. 2a). Deletion and point mutations associated with *daf-16* alleles (see below) were localized within cosmid R13H8 to a gene that encodes a member of the Fork head family of transcription factors. The *daf-16*(*mgDf50*) null allele (see below) was rescued by injection of cosmid R13H8 into the germ line of a *daf-16*(*mgDf50*);*daf-2*(*e1370*) double mutant and showing that transgenic progeny arrest at the dauer stage. A neighbouring cosmid did not rescue this *daf-16* mutant allele.

Analysis of *daf-16* cDNAs revealed three alternatively spliced forms, designated *daf-16a1*, *daf-16a2* and *daf-16b* (Fig. 2a). DAF-16a and DAF-16b have distinct, but highly related, Fork head type DNA-binding domains (73% identical (87/119 amino acids); Fig. 2c). The amino-terminal half of the DNA-binding domain is encoded by exons 3 and 4 for DAF-16a and exon 5 for DAF-16b. The C-terminal half of each DNA-binding domain is encoded by exons 6 and 7 which are common to both transcripts (Fig. 2). Two similar isoforms of DAF-16a, DAF-16a1 and DAF-16a2 are encoded by the same 11 exons, except that exon 3 is alternatively spliced, resulting in the addition of two amino acids to DAF-16a1 outside the DNA-binding domain (Fig. 2a, b).

The DAF-16a and DAF-16b isoforms are probably generated from distinct promoters, suggesting that they could be expressed in and mediate DAF-2 signalling in distinct tissues or cell types (see below). These isoforms have distinct Fork head DNA-binding domains that may interact with distinct partners (for example, DAF-3, DAF-8 or DAF-14; see below) or may bind to distinct downstream promoters. Significantly, the probable DNA-binding specificity determinant of Fork head proteins in helix 3 (ref. 3) is common to the DAF-16 isoforms. Thus, the expression and differential splicing of the two distinct DAF-16 Fork head DNA-binding domains is expected to be functionally important but is not obviously implicated in DNA-binding specificity.

The most closely related proteins in GenBank to DAF-16 are human FKHR and AFX (Fig. 2c, d). Within the Fork head DNA-binding domain, DAF-16a is 65% identical (78/120) to FKHR and 62% identical (74/120) to AFX. DAF-16b is 50% identical (60/120) to FKHR and 47% identical (56/120) to AFX. Within this region, FKHR and AFX are 81% identical (95/117). In addition, there is a region at the amino-terminal end of each protein that is 55% identical (10/18) between DAF-16a and FKHR and AFX. This region is not conserved between other Fork head-related proteins

nor between DAF-16b and FKHR or AFX. DAF-16a is only 36% identical to Freac-4 and DAF-16b is only 33% identical to Freac-3 (Fig. 2d), which are the next most closely related proteins in the GenBank or dbEST databases. DAF-16a and DAF-16b are similarly distinct from the closest *C. elegans* homologues (Fig. 2d). Phylogenetic tree analysis of the Fork head domain of DAF-16 and its closest relatives show that FKHR, AFX and DAF-16 constitute a distinct class (Fig. 2d).

The high degree of sequence similarity suggests that FKHR and AFX may correspond to the human orthologues of DAF-16 and constitute major transcriptional outputs of insulin or IGF-1 receptors in mammals. FKHR and AFX, however, were identified as oncogene breakpoints and not, like DAF-16, as metabolic transcriptional regulators. The oncogenic translocations fuse a disrupted FKHR or AFX Fork head DNA-binding domain and intact carboxy-terminal activation domain to other DNA-binding domains[10,11]. The PAX-3/FKHR fusion protein is a more potent transcriptional activator than PAX-3 (ref. 12). Although FKHR and AFX activities are not yet known to be regulated by insulin or IGF, growth of rhabdomyosarcomas is suppressed by declines in IGF-1 receptor signalling[13,14] and these tumours accumulate large amounts of glycogen[15]. The HNF3 Fork head transcription factor has been implicated in insulin regulation of metabolic gene transcription[16]. Because distantly related Fork head proteins bind to similar sites[17], HNF3-binding *cis*-acting sites from insulin-responsive metabolic control genes may actually be regulated by the FKHR or AFX protein in mammals. Non-null mutations in FKHR or AFX that decouple these transcription factors from the insulin signalling cascade may underlie type II diabetes in some pedigrees.

Identification of *daf-16* null alleles establishes that the most

Figure 2 *daf-16* encodes a Fork head/HNF3-related transcription factor. **a**, Top, genetic and physical map of the *daf-16* region, bottom, exon/intron structure of *daf-16*. Coding regions are filled boxes, non-coding regions are open boxes, and introns are lines. The Fork head regions are indicated in grey. **b**, Molecular identity of six mutations identified in *daf-16*. The genomic region of *daf-16* is shown. Boxes indicate exons, and areas in grey indicate regions homologous to the Fork head domain. Two point mutants (*mg54* and *mg53*) are shown simply as arrows pointing to the location of the lesion (see also **c**). Two point mutants (*m26* and *mg87*) affect splice sites and are shown below. The extent of the *mgDf47* and *mgDf50* deletions is indicated. The area between the vertical lines is deleted, and areas of uncertainty are indicated by dotted lines. **c**, DNA-binding domains of DAF-16a, DAF-16b and human FKHR (U02310), AFX (X93996) and HNF3α were aligned using Pileup (GCG). Amino acids that are identical in at least three of the proteins are highlighted. Horizontal arrow indicates the beginning of exon 6 which is shared between DAF-16a and DAF-16b. Point mutations within the DNA-binding domains of DAF-16 are indicated; *daf-16*(*mg54*) is specific for DAF-16a, whereas *daf-16*(*mg53*) is common for both DAF-16a and DAF-16b. Vertical arrow indicates the fusion point for the PAX-3/FKHR and HTRX1/AFX-1 fusion proteins that are caused by chromosomal translocations found in human tumours. **d**, Pileup (GCG) was used to align the DNA binding domains of the listed proteins. Human proteins are indicated in bold text and *C. elegans* proteins are indicated by plain text. C47G2.2 is a gene-finder-predicted ORF on cosmid C47G2. The accession numbers for the daf-16 sequences are AF020342 daf-16a1; AF020343 daf-16a2 and AF020344 daf-16b.

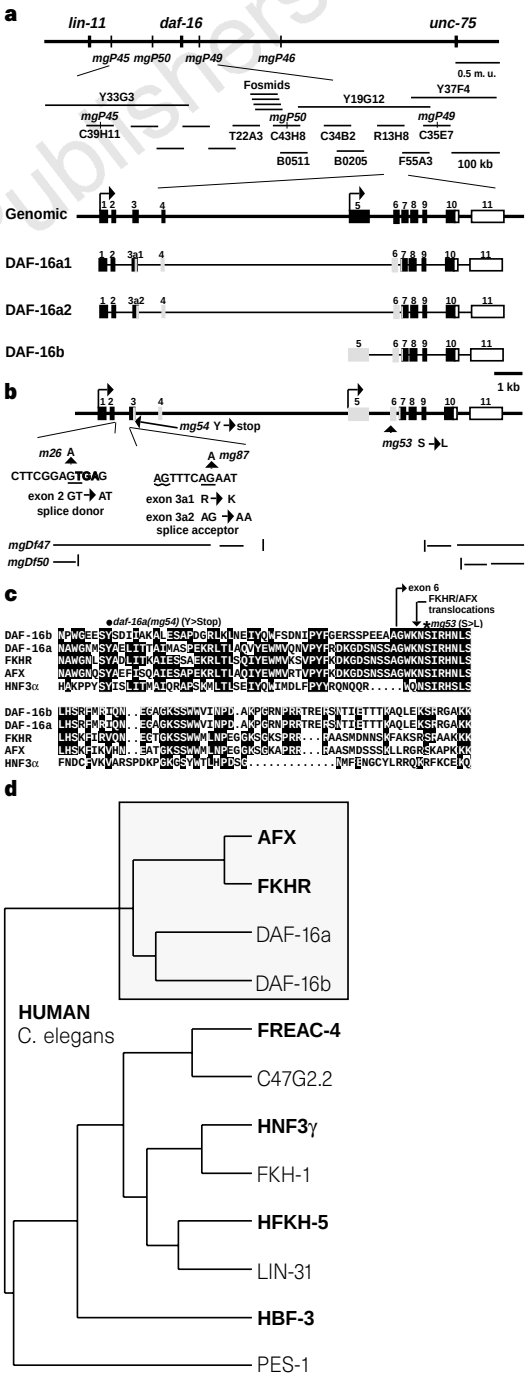

Table 2 Synergy of insulin receptor-like and TGF-β receptor-like signalling

Genotype	% Dauer formation		
	15 °C	18 °C	20 °C
daf-2(*e1370*)	0 (n = 611)	5 (n = 487)	5 (n = 506)
daf-1(*m40*)	0 (n = 434)	0 (n = 732)	1 (n = 909)
daf-2(*e1370*); *daf-1*(*m40*)	17 (n = 652)	99 (n = 861)	100 (n = 718)

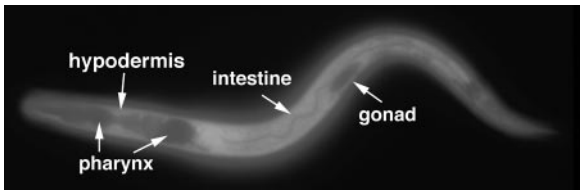

Figure 3 Expression of a *daf-16a*::*GFP* fusion gene in an L1 animal.

important *daf-16* function is in dauer arrest and metabolic regulation. *daf-16*(*mgDf47*) and *daf-16*(*mgDf50*) were isolated after γ-ray mutagenesis and are molecular null alleles that delete conserved domains or nearly all of the *daf-16* coding region (Fig. 2b). As already described, both of these *daf-16* null alleles have the same phenotypes: viable and complete suppression of the *daf-2* dauer constitutive and energy storage phenotypes.

Molecular analysis of other *daf-16* mutant alleles revealed that the two major DAF-16 isoforms are not redundant. *daf-16*(*mg54*) is an amber stop mutation within the DNA-binding domain of DAF-16a but is predicted not to affect DAF-16b (Fig. 2b, c). *daf-16*(*mg54*) suppresses the dauer constitutive phenotype caused by *daf-2* mutations (Table 1). Two other *daf-16* alleles, *m26* and *mg87*, are also specific to the *daf-16a* isoform (Fig. 2c). *daf-16*(*m26*) incompletely suppresses *daf-2*(*e1370*) (ref. 7). The identification of *daf-16a*-specific mutations indicates that *daf-16b* activity is not sufficient to induce dauer arrest in a *daf-2* mutant. No mutation that is specific for the *daf-16b* Fork head region was detected in a collection of 11 *daf-16* alleles sequenced, so it is not known if this isoform is necessary for *daf-2* and *age-1* induced dauer arrest. The only point mutation that affects both *daf16* isoforms, *daf-16*(*mg53*), changes a conserved serine in the Fork head DNA-binding domain to leucine (Fig. 2b, c).

Arrest at the dauer larval stage affects the morphology and metabolism of many *C. elegans* tissues[3]. DAF-16 might act directly in these target tissues or indirectly in neuronal or other signalling cells that in turn regulate the development and metabolism of target tissues. *daf-16* expression was addressed using a *daf-16a*::green fluorescent protein (GFP) fusion gene. Transgenic *daf-16a*::*GFP* animals show strong GFP fluorescence in most cells including ectoderm, muscles, intestine and neurons (Fig. 3). The broad expression pattern of *daf-16a*::*GFP* is also seen in late embryos, larvae and dauer larvae. No expression was seen in the pharynx even though the morphology of the pharynx is altered in dauer larvae, and *daf-16* gene activity is essential for this pharyngeal change in pheromone (Table 1) or *daf-7*-induced dauers[7]. It is possible that *daf-16b* is expressed in the pharynx and serves this function, that the *daf-16a*::*GFP* fusion gene does not bear those regulatory sequences, or that *daf-16* acts non-autonomously to affect the pharynx.

The expression of *daf-16a* in the many target tissues that are metabolically and developmentally shifted in dauers is consistent with its action in target tissues to regulate dauer arrest, metabolism and longevity. In addition to the metabolic changes that occur in dauer larvae, some tissues are remodelled or developmentally arrested. The hypodermis shrinks and stores fat. The intestinal lumen is shrunken and becomes refractile. The collagen composition of the cuticle is altered by changes in the expression of collagen genes[3]. *daf-16* is expressed in all of these tissues, suggesting that these phenotypic changes, including the metabolic shifts, may be induced by DAF-16-responsive genes.

daf-2 and *age-1* mutations also cause an increase in lifespan[2,4,5,18]. These effects are suppressed by *daf-16* mutations[4,5,18]. Thus DAF-16 might directly regulate the genes necessary for increased longevity. For example, dauer larvae express higher superoxide dismutase levels, which might protect them from oxygen radicals[19]. This gene may be directly regulated by DAF-16. The suppression of the longevity increases of *daf-2* and *age-1* mutants by *daf-16* mutations suggests that other outputs of the DAF-2/AGE-1 signalling pathway, for example the regulation of glucose transport or metabolic enzyme activities, are not relevant to lifespan or dauer arrest in the absence of DAF-16 transcriptional regulation.

In extensive genetic screens for *daf* mutants, the only suppressors of *daf-2* that have been identified are *daf-16* (many alleles)[6,20] and *daf-18* (one allele)[20]. Therefore, *daf-16* is likely to represent the principal negatively regulated output of this insulin receptor-like signalling pathway. The lack of other *daf-2* suppressors argues against the existence of another entire ligand/receptor signalling pathway between *daf-2* and *daf-16* and suggests that *daf-16* acts in the same cell as *daf-2*.

The finding that DAF-16 encodes proteins highly related to the Fork head class of transcription factors suggests a molecular model for the negative regulation of DAF-16 by upstream DAF-2/AGE-1 signalling (Fig. 4). DAF-2 insulin receptor-like engagement by an unidentified ligand activates the AGE-1 phosphatidylinositol–3-OH kinase (PI(3)K). In mammals, PI(3)K signalling activates protein kinase cascades, including the AKT/PKB kinase[21] that regulates metabolic enzyme activities as well as glucose transport[22]. We suggest that the homologous DAF-2/AGE-1 regulated kinase cascade couples to the DAF-16 transcription factor (as well as to metabolic enzymes and transporters). We suggest that in the absence of DAF-2/AGE-1 signalling inputs, DAF-16 acts as a repressor of metabolic genes that mediate energy usage (Fig. 4b). The repression of these genes causes a metabolic shift to energy storage that can be relieved by loss of *daf-16* gene activity. When the DAF-2/AGE-1 signalling cascade is activated under reproductive growth conditions, we suggest that a kinase cascade leads to the modification of the transcriptional activity of DAF-16 (Fig. 4a). This signalling may either change DAF-16 to an activator (Fig. 4a) or inactivate DAF-16 repressor function to now allow the expression of metabolic genes necessary for reproductive development.

There is precedent for the model that DAF-16 transcriptional activity is modulated by upstream tyrosine kinase signals: in *C. elegans* vulval cell lineages, the activity of the LET-23 EGF receptor kinase is coupled to the activity of the LIN-31 Fork head transcription factor (P. Tan and S. Kim, personal communication). And similar to the suppression of *daf-2* mutant phenotypes by *daf-16* null mutations, *lin-31* mutations bypass the normal requirement of upstream LET-23 EGF-like receptor signalling for the execution of particular vulval cell lineages[23].

In addition to the DAF-2/DAF-16 pathway, the activity of the parallel DAF-7 TGF-β pathway also regulates *C. elegans* metabolism. We find genetic synergy between the DAF-2 and DAF-7

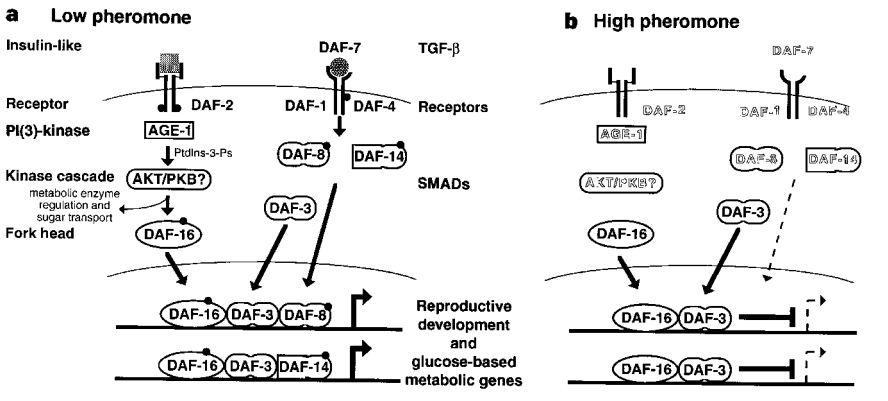

Figure 4 Model for regulation of dauer formation by convergent transcriptional outputs from insulin receptor-like and TGF-β-like signal transduction pathways. **a**, Reproductive development occurs in low pheromone as a result of high DAF-2 ligand and DAF-7 signals. **b**, Dauer formation occurs when high pheromone levels downregulate DAF-2 ligand and DAF-7 signals.

signalling pathways by comparing the phenotype of a *daf-2*; *daf-1* double mutant to the phenotype of each single mutant (Table 2). This synergy, together with the similar phenotypes of mutants in the two pathways, implies that the pathways cooperate to control reproductive versus dauer development and metabolism. DAF-7 TGF-β is expressed by the exposed sensory neuron ASI under conditions that induce reproductive development but not in dauer pheromone.[24] Mutations that decrease or eliminate DAF-7 activity or the activities of the type I receptor DAF-1 (ref. 25) and type II receptor DAF-4 (ref. 26), or probable downstream SMAD proteins DAF-8 (A. Estevez and D. L. Riddle, personal communication), and DAF-14 (T. Inoue and J. Thomas, personal communication) cause arrest at the dauer stage and a metabolic shift to fat storage (Fig. 2). The dauer constitutive and fat storage phenotypes caused by mutations in these upstream TGF-β signalling genes are suppressed by null mutations in *daf-3*, which also encodes a SMAD protein[8] (Fig. 2). Thus *daf-3* acts in this TGF-β pathway analogously to *daf-16* in the insulin-like pathway: *daf-3* gene activity is negatively regulated by upstream TGF-β signalling.

Similar convergence between tyrosine kinase receptor-mediated and TGF-β-related signalling pathways has been noted in early vertebrate development[27]. Precedent from the regulation of *Xenopus* early development by activin/Smad2 signalling suggests a molecular model for convergent insulin receptor tyrosine kinase and TGF-β receptor regulation of development and metabolism: the Fork head protein FAST1 directly interacts with Smad2 cooperatively to bind to an activin-response element on a gene that is transcriptionally regulated by activin[28]. The synergy between mutations in the *daf-2* insulin receptor-like and *daf-1* TGF-β receptor suggests that insulin-like transducing DAF-16 may interact with the TGF-β signal transducing SMAD proteins DAF-3, DAF-8 and/or DAF-14 on the promoters of genes that regulate metabolism and reproductive versus dauer development (Fig. 4).

We suggest that under low-pheromone conditions, when both DAF-2 ligand and DAF-7 endocrine signals are produced, DAF-16 activity is modified by an upstream DAF-2/AGE-1 kinase cascade, and DAF-8 and DAF-14 are phosphorylated by upstream DAF-7/DAF-1/DAF-4 receptor kinase signalling to induce a heteromeric Fork head/SMAD transcription factor complex (Fig. 4a). The complex activates expression of genes that mediate reproductive growth and metabolism. Under dauer-inducing conditions, we suggest that a low level of DAF-2 ligand does not activate phosphorylation of DAF-16 by the DAF-2/AGE-1 signalling cascade, and a low level of DAF-7 TGF-β does not activate phosphorylation of DAF-8 and DAF-14 by the DAF-1/DAF-4 receptor kinases. In these dauer-inducing conditions, we suggest that DAF-16 and DAF-3 form heteromers that repress the expression of reproductive development and metabolic genes.

Because *daf-3* (ref. 8), *daf-4* (ref. 8) and *daf-16* GFP fusion genes are widely expressed, we suggest that the integration of DAF-2 insulin receptor-like and DAF-7 TGF-β signalling takes place in the target tissues where the metabolic shifts are noted (Figs 1 and 4). The genes regulated by the Fork head/SMAD transcriptional regulatory complex may correspond to the *C. elegans* homologues of mammalian genes, such as those that encode PEPCK and the Glut4 glucose transporter, which are transcriptionally regulated by insulin[29]. However, the molecular model does not depend on the signal integration taking place in target tissues. The signals may converge only in key regulatory cells, which in turn generate signals that regulate target tissue metabolism and development. In such a case, the downstream genes whose transcription is regulated by DAF-16 and DAF-3, DAF-8 and DAF-14 would not be target-tissue metabolic-control genes analogous to those regulated by insulin, but rather genes that encode other endocrine hormones.

It may be significant to the development of treatments for diabetes that *C. elegans* carrying mutations in *daf-16* can grow reproductively even if they also carry *daf-2* mutations that disable insulin-receptor-like metabolic-control signals (Table 1). Thus the genetics yield the surprising result that these animals can live normally without insulin-receptor-like signalling if they are also mutant in *daf-16*. Some of the human metabolic defects that result from declines in insulin signalling in both type I and type II diabetes may be caused by unregulated activity of the human DAF-16 orthologues FKHR and AFX, in turn to cause changes in the expression of metabolic control enzymes. Inhibition of FKHR or AFX activities, for example by pharmaceutical agents that inhibit DNA binding or association with transcriptional partners, may ameliorate the metabolic defects caused by declines in insulin signalling. The more acute insulin responses, for example in glucose uptake and in metabolic enzyme activities, would not be directly affected by these transcriptional regulators.

The molecular model for convergent insulin-like and TGF-β signalling suggests that these pathways meet on the promoters of metabolic-control genes. Given such a mechanistic connection between the *C. elegans* insulin-like and TGF-β transcriptional outputs, this molecular complex may be conserved across phylogeny. We propose that, as in *C. elegans*, both insulin and a DAF-7-like neuroendocrine signal may be necessary for metabolic control in humans. Accordingly, the failure of target tissues to respond to insulin signals in type II diabetic patients could be due to defects in either the insulin or TGF-β signalling pathways. Genetic predisposition to type II diabetes has been noted. Declines in signalling from the human orthologues of DAF-7 (or in any of the signalling molecules downstream of DAF-7), could underlie the lack of response to insulin in type II diabetes, just as lack of DAF-7 signalling in *C. elegans* causes very similar metabolic defects as lack of DAF-2 signalling. Obesity is a major risk factor in type II diabetes. One attractive model for the connection between obesity and insulin signalling defects is that metabolic signals analogous to the dauer pheromone, which may be a fatty acid[30], or hormonal signals from fat cells may downregulate production of human DAF-7. □

Methods

***daf-16* molecular genetics.** DNA segments from the gap in the cosmid coverage of the *daf-16* genetic region were identified by probing a fosmid library with the end of cosmid T22A3, which defined the left endpoint of the gap that contains *daf-16*. One end of each fosmid so identified was identical to nucleotide sequence of two overlapping cosmids (C43H8 and B0511) near the end of a previously unlocalized 300 kb contig. Cosmids or PCR products from genomic sequence distributed along the length of this contig were used to detect RFLPs between *C. elegans* strains Bristol N2 and Bergerac RC301 (*mgP45* on cosmid C39H11, *mgP46* on cosmid F28D9, *mgP49* on cosmid C35E7, and *mgP50* on cosmid C43H8). These RFLP loci were mapped relative to the *lin-11 daf-16 unc-75* genetic interval. Thirty-three Daf non-Unc recombinants from a *daf-16*(*m27*) *unc-75*(*e950*); *daf-2*(*e1370*)/*daf-16*(+*RC301*) *unc-75*(+*RC301*) strain and four Daf non-Lin recombinants from the strain *lin-11*(*n566*) *daf-16*(*m27*); *daf-2*(*e1370*)/*lin-11*(+*RC301*) *daf-16*(+*RC301*) were recovered. In the Daf non-Unc class, 13/33 recombinant chromosomes carried the Bergerac RC301 of RFLP *mgP46*, 2/30 recombinant chromosomes carried the Bergerac RC301 allele of *mgP49*, and 0/11 and 0/2 carry the Bergerac RC301 allele of RFLP *mgP45* and *mgP50*. In the Daf non-Lin class, 3/4 of the recombinant chromosomes carried the Bergerac RC301 of RFLP *mgP45* and 0/4 of the recombinant chromosomes carried the Bergerac RC301 allele of *mgP49*. *daf-16*(*mgDf50*); *daf-2*(*e1370*) animals were injected with 100 ng μl^{-1} pRF4 and 5 ng μl^{-1} of either cosmid R13H8 or B0205. The extent of the deficiencies associated with *daf-16*(*mgDf47*) and *daf-16*(*mgDf50*) were further characterized by PCR and Southern blotting. To characterize point mutations, genomic DNA from *daf-16*(*mg53*), *daf-16*(*mg54*), *daf-16*(*m26*), *daf-16*(*mg87*) and other *daf-16* mutant alleles was PCR-amplified and directly sequenced.

Assaying dauer formation. Characterization of *daf-16* null and *daf-3* null suppression of *daf-2*: synchronized egg broods were grown at 25 °C and scored ~48 h later. Numbers represent totals from 7 or 8 trials for each genotype performed on two different days. Assays for dauer formation on pheromone

were done as described[30]. Genetic synergy between *daf-1* and *daf-2*: synchronized egg broods were scored at ~48 h and rescored at ~72 h for 25 °C trials, at about 66 and 90 h for both 18 °C and 20 °C trials, or at ~95 and 120 h for 15 °C trials. Numbers in Table 1 represent the summary of five trials of each genotype in two experiments performed on different days.

Expression of *daf-16*. A *daf-16a*::GFP fusion was constructed in the following manner. The *daf-16a* promoter region containing ~6.0 kb of genomic DNA upstream of the *daf-16* 5′ UTR and including the 5′ UTR and most of exon 1 from *daf-16* was PCR-amplified using primers containing the appropriate restriction sites. This genomic fragment was digested with *Sma*I and *Bam*HI and ligated to pPD95.75 (gift from A. Fire) digested with *Sma*I and *Bam*HI. The *daf-16a*::GFP plasmid was injected at 50 ng μl^{-1}, together with pRF4 at 100 ng μl^{-1}.

Received 20 August; accepted 2 October 1997.

1. Kimura, K. D. *et al*. *daf-2*, an insulin receptor-like gene that regulates longevity and diapause in *Caenorhabditis elegans*. *Science* **277,** 942–946 (1997).
2. Morris, J. Z., Tissenbaum, H. A. & Ruvkun, G. A phosphatidylinositol-3-OH kinase family member regulating longevity and diapause in *Caenorhabditis elegans*. *Nature* **382,** 536–539 (1996).
3. Riddle, D. L. Genetic and environmental regulation of dauer larva development in *C. elegans* II, (eds Riddle, D. L. *et al.*) 739–768 (Cold Spring Harbor Press, NY, 1997).
4. Kenyon, C. *et al*. A *C. elegans* mutant that lives twice as long as wild type. *Nature* **366,** 461–464 (1993).
5. Larsen, P. L., Albert, P. S. & Riddle, D. L. Genes that regulate both development and longevity in *Caenorhabditis elegans*. *Genetics* **139,** 1567–1583 (1995).
6. Gottlieb, S. & Ruvkun, G. daf-2, daf-16, and daf-23: Genetically interacting genes controlling dauer formation in *C. elegans*. *Genetics* **137,** 107–120 (1994).
7. Vowels, J. J. & Thomas, J. H. Genetic analysis of chemosensory control of dauer formation in *Caenorhabditis elegans*. *Genetics* **130,** 105–123 (1992).
8. Patterson, G. I. *et al*. A Smad protein that acts antagonistically in the *C. elegans* TGF-β dauer regulatory pathway. *Genes Dev.* (in the press).
9. Clark, K. L. *et al*. Co-crystal structure of the HNF-3/fork head DNA-recognition motif resembles histone H5. *Nature* **364,** 412–420 (1993).
10. Galili, N. *et al*. Fusion of a fork head domain to PAX-3 in the solid tumor alveolar rhabdomyosarcoma. *Nature Genet.* **5,** 230–235 (1993).
11. Borkhardt, A. *et al*. Cloning and characterization of AFX, the gene that fuses to MLL in acute leukemias with a t(X;11)(q13;q23). *Oncogene* **14,** 195–202 (1997).
12. Federicks, W. J. *et al*. The PAX3-FKHR fusion protein created by the t(2;13) translocation in alveolar rhabdomyosarcomas in a more potent transcriptional activator than PAX3. *Mol. Cell. Biol.* **15,** 1522–1535 (1995).
13. Kalebic, T., Tsokos, M. & Helman, L. J. *In vivo* treatment with antibody against IGF-1 receptor suppresses growth of human rhabdomyosarcoma and down-regulates $p34^{cdc2}$. *Cancer Res.* **54,** 5531–5534 (1994).
14. Shapiro, D. N. *et al*. Antisense-mediated reduction in insulin-like growth factor-I receptor expression suppresses the malignant phenotype of a human alveolar rhabdomyosarcoma. *J. Clin. Invest.* **94,** 1235–1242 (1994).
15. Nojima, T. *et al*. A case of alveolar rhabdosarcoma with a chromosomal translocation, t(2;13)q37;q14). *Virchows Arch. Path.* **417,** 357–359 (1990).
16. Lai, E. *et al*. HNF-3A, a hepatocyte-enriched transcription factor of novel structure is regulated transcriptionally. *Genes Dev.* **4,** 1427–1436 (1990).
17. Kaufmann, E., Muller, D. & Knochel, W. DNA recognition site analysis of *Xenopus* winged helix proteins. *J. Mol. Biol.* **248,** 239–254 (1995).
18. Dorman, J. B. *et al*. The *age-1* and *daf-2* genes function in a common pathway to control the lifespan of *Caenorhabditis elegans*. *Genetics* **141,** 1399–1406 (1995).
19. Larsen, P. Aging and resistance to oxidative damage in *Caenorhabditis elegans*. *Proc. Natl Acad. Sci. USA* **90,** 8905–8909 (1993).
20. Riddle, D. L., Swanson, M. M. & Albert, P. S. Interacting genes in nematode dauer larva formation. *Nature* **290,** 668–671 (1981).
21. Toker, A. & Cantley, L. C. Signalling through the lipid products of phosphoinositide-3-OH kinase. *Nature* **387,** 673–676 (1997).
22. Tanti, J. F. *et al*. Overexpression of a constitutively active form of phosphatidylinositol 3-kinase is sufficient to promote Glut4 translocation in adipocytes. *J. Biol. Chem.* **271,** 25227–25232 (1996).
23. Miller, L. M. *et al*. *lin-31*, a *Caenorhabditis elegans* HNF-3/fork head transcription factor homolog, specieis three alternative cell fates in vulval development. *Genes Dev* **7,** 933–947 (1993).
24. Ren, P. *et al*. Control of *C. elegans* larval development by neuronal expression of a TGF-β homologue. *Science* **274,** 1389–1391 (1996).
25. Georgi, L. L., Albert, P. S. & Riddle, D. L. *daf-1*, a *C. elegans* gene controlling dauer larva development, encodes a novel receptor protein kinase. *Cell* **61,** 635–645 (1990).
26. Estevez, M. *et al*. The *daf-4* gene encodes a bone morphogenetic protein receptor controlling *C. elegans* dauer larva development. *Nature* **365,** 644–649 (1993).
27. Green, J. B., New, H. V. & Smith, J. C. Responses of embryonic *Xenopus* cells to activin and FGF are separated by multiple dose thresholds and correspond to distinct axes of the mesoderm. *Cell* **71,** 731–739 (1992).
28. Chen, X., Rubock, M. J. & Whitman, M. A transcriptional partner for MAD proteins in TGF-β signalling. *Nature* **383,** 691–696 (1996).
29. O'Brien, R. M. *et al*. Hepatic nuclear factor 3- and hormone-regulated expression of the phosphoenolpyruvate carboxykinase and insulin-like growth factor-binding protein 1 genes. *Mol. Cell. Biol.* **15,** 1747–1758 (1995).
30. Golden, J. W. & Riddle, D. L. A pheromone influences larval development in the nematode *Caenorhabditis elegans*. *Science* **218,** 578–580 (1982).

Acknowledgements. We thank S. Chissoe, A. Coulson and the *C. elegans* genome sequencing consortium for sending clones and information and for their help; Y. Liu and F. Lam for technical assistance; Y. Kohara for cDNA clones; R. Barstead for the RB1 and RB2 cDNA libraries; and members of G.R.'s laboratory for discussion and for comments on the manuscript. Some of the strains were provided by the *C. elegans* Genetics Center which is supported by the national Center for Research Resources. This work was supported by a grant from the NIH.

Correspondence and requests for materials should be addressed to G.R. (e-mail: ruvkun@opal.mgh.harvard.edu).

Structure of the cyclin-dependent kinase inhibitor $p19^{Ink4d}$

Frederich Y. Luh*, Sharon J. Archer†, Peter J. Domaille†, Brian O. Smith*, Darerca Owen*, Deborah H. Brotherton*, Andrew R. C. Raine*, Xu Xu‡, Leonardo Brizuela‡, Stephen L. Brenner† & Ernest D. Laue*

** Cambridge Centre for Molecular Recognition, Department of Biochemistry, University of Cambridge, Tennis Court Road, Cambridge CB2 1QW, UK*
† Du Pont Merck Pharmaceutical Company, Box 80328, Wilmington, Delaware 19880-0328, USA
‡ Mitotix Inc., One Kendall Square, Building 600, Cambridge, Massachusetts 02139, USA

In cancer, the biochemical pathways that are dominated by the two tumour-suppressor proteins, p53 and Rb, are the most frequently disrupted. Cyclin D-dependent kinases phosphorylate Rb to control its activity and they are, in turn, specifically inhibited by the Ink4 family of cyclin-dependent kinase inhibitors (CDKIs) which cause arrest at the G1 phase of the cell cycle. Mutations in Rb, cyclin D1, its catalytic subunit Cdk4, and the CDKI $p16^{Ink4a}$, which alter the protein or its level of expression, are all strongly implicated in cancer. This suggests that the Rb 'pathway' is of particular importance[1]. Here we report the structure of the $p19^{Ink4d}$ protein, determined by NMR spectroscopy[2–4]. The structure indicates that most mutations to the $p16^{Ink4a}$ gene, which result in loss of function, are due to incorrectly folded and/or insoluble protein[5]. We propose a model for the interaction of Ink4 proteins with D-type cyclin-Cdk4/6 complexes that might provide a basis for the design of therapeutics against cancer.

The sequences of the Ink4 family of CDKIs are highly conserved (Fig. 1): there are at present four known family members, $p15^{Ink4b}$, $p16^{Ink4a}$, $p18^{Ink4c}$ and $p19^{Ink4d}$. In contrast to the p21/p27/p57 family of CDKIs, which inhibit a broad range of CDKs, the Ink4 family is specific for Cdk4 and Cdk6 (refs 4, 6). The Ink4 proteins, which consist of four or more ankyrin repeats[7], are expressed in distinct tissue-specific patterns, suggesting that although they have essentially indistinguishable biochemical properties[4], they are not strictly redundant[1]. $p15^{Ink4b}$ is induced in human keratinocytes in response to the transforming growth factor TGF-β (ref. 8). Consistent with its role as a potent inhibitor of Rb phosphorylation, $p16^{Ink4a}$ is altered in familial melanomas[9], and $Ink4a^{-/-}$ mice spontaneously develop tumours[10]. In addition, methylation of the 5′ CpG island is associated with transcriptional silencing of $p16^{Ink4a}$ in human cancers[11]. Both $p18^{Ink4c}$ and $p19^{Ink4d}$ are periodically expressed in proliferating macrophages (maximally during the S-phase of the cell cycle), suggesting that they might limit cyclin-D-dependent kinase activity once cells exit the G1 phase[4].

Intact mouse $p19^{Ink4d}$ protein was purified from *Escherichia coli* following coexpression with the chaperone proteins GroEL and GroES[12]. The recombinant $p19^{Ink4d}$ protein was able to inhibit cyclin D1/Cdk4 at similar concentrations to $p16^{Ink4a}$ (ref. 13, and data not shown). We found that $p16^{Ink4a}$ and $p19^{Ink4d}$ were equally defective in binding an R24C mutant of Cdk4 (ref. 14, and data not shown). These results are consistent with others suggesting that the two proteins have indistinguishable biochemical activities[4]. However, $p19^{Ink4d}$ aggregated less and gave better NMR spectra than $p16^{Ink4a}$ at the high concentrations required for structural studies. ^{1}H, ^{13}C and ^{15}N chemical shifts of $p19^{Ink4d}$ were assigned after recording three- and four-dimensional (3D, 4D) double and triple resonance NMR spectra of ^{15}N- and $^{13}C/^{15}N$-labelled proteins. The elements of secondary structure (Fig. 1) were identified from the Cα and Cβ